Acta Acustica united with Acustica
Vol. 101 (2015) 1211 – 1221
DOI 10.3813/AAA.918914

Modal Energy Analysis of Nearly Rectangular Rooms at Low Frequencies

Jens Holger Rindel
Multiconsult AS, Oslo, Norway. jehr@multiconsult.no

Summary
This paper describes a method where the normal modes of a rectangular room are analysed as independent resonant systems with internal losses derived from the absorption properties of the room surfaces. Thus the resonance frequency, the bandwidth, and the decay rate of each normal mode can be calculated. A new method using a representative wave has been applied to calculate the decay rate of a normal mode. By adding the frequency responses of all normal modes up to a sufficiently high order the global frequency response below 200 Hz is found. The decay curve within a frequency band can be calculated by adding together the individual decay curves of the relevant modes. Typically the axial modes have longer reverberation times than tangential and oblique modes, and thus the total decay curve will not be a perfectly straight line. The effect of angled walls or scattering treatment of surfaces is modelled in terms of modal energy analysis, the most important result being that sound energy is transferred from the powerful axial modes to other modes with less energy, and thus leading to a shorter reverberation time. A new theoretical model for energy losses of axial modes due the scattering or angled walls is presented. The presented model using modal energy analysis is suggested as a tool for the analysis and design of small music practice rooms and recording studios.
PACS no. 43.55.Br, 43.55.Fw, 43.55.Ka

1. Introduction

In small rooms such as music practice rooms and recording studios a smooth frequency response in the low frequency range is important for the acoustical quality. For the acoustical design it is a well-established practice to avoid room dimensions that are equal or in simple proportions and to recommend non-parallel walls. However, the existing design tools for this kind of rooms are either too simple to provide reliable results – like the rule-of-thumb that a wall should be turned a certain angle – or too complicated and time consuming to be applied in practice – like FEM and BEM models.

The ratio between length, width and height of a room is crucial for obtaining an even frequency distribution of the modes at low frequencies. Proposals for optimum room dimensions have been the topic of many papers since the early days of room acoustics. In 1942 Volkman [1] suggested different ratios based on the $\sqrt[3]{2}$ and presented a diagram with recommended ratios for different room sizes, e.g. 1:1.25:1.6 for small rooms and 1:1.6:2.5 for average sized rooms. He also mentioned the ratio 2:3:5 to be frequent practice in the broadcast field.

Bolt [2] suggested a range of usable ratios displayed as a design chart. Lyon [3] found the optimum ratio to be 1:0.8:0.63, i.e. in reality the same as Volkman [1]. Louden [4] looked at the distribution of the natural frequencies and calculated the deviation from the statistical distribution in order to rank good dimension ratios, and he found 1:1.4:1.9 to be the best one. Bonello [5] suggested a criterion based on the number of natural frequencies per third octave band between 10 and 200 Hz, and this should increase monotonically with centre frequency in a good room. He also noted that the room volume is an important parameter, so there is no optimum dimension ratio covering all volumes. Cox and D'Antonio [6] applied an image source model with source in one corner and receiver in the opposite corner to calculate the frequency response. By numerical optimisation the room dimensions were changed to achieve the flattest possible frequency response in the frequency range 20–200 Hz. They reported the worst case ratio within a given search range to be (1:1.075:1.868), but they did not report the actual optimized dimension ratios. Instead calculated frequency responses were shown in comparison with results for some of the above mentioned recommendations, (2:3:5), (1:1.4:1.9), (1:1.26:1.59), and the golden ratio. In all cases the optimized proportions gave a frequency response with less deviation from a flat curve.

The first part of this paper deals with calculation of frequency response and reverberation time at low frequencies (20–200 Hz) in small rectangular rooms. Usually the frequency response is measured as the transfer function between two points in the room. However, for the design of a music room or other rooms where the positions of source and receiver are not well defined, it may be suffi-

Received 12 December 2014,
accepted 30 June 2015.

© S. Hirzel Verlag · EAA

cient to consider the total energy in the room as a function of the frequency, and this is named the *global frequency response*. In the design of a room it may be both an advantage and a simplification that the choice of source and receiver positions is excluded in the acoustical analysis.

Assuming a broadband excitation, the reverberation time and the steady-state energy in each room mode are calculated from the absorption coefficients of the surfaces. A *representative wave path* is used for this derivation. Thus, the frequency response of each mode is known, and the responses for all relevant modes can be added together to give the global frequency response of the room. With the focus on the low frequencies (20–200 Hz) in small rooms, it is sufficient to include modes up to a certain number in the analysis, e.g. 9th order, which yields $10^3 = 1000$ modes including the first pressure chamber mode (0, 0, 0). This number of modes is sufficient to cover the low frequency range up to 200 Hz for room dimensions up to 8.5 m.

At low frequencies the reverberation time is highly frequency dependent, being rather long in axial modes and much shorter in tangential and oblique modes. The reason for this is simply that the average path between reflections is longest in the axial modes and shortest in the oblique modes. So, even with the same absorption coefficient on all surfaces, the axial modes have the lowest attenuation per time unit, while the oblique modes have the highest attenuation. This can be further exaggerated if the sound absorption is unevenly distributed on the surfaces, which is often the case. Within a certain frequency band, e.g. the 63 Hz octave band, the decay curves of each mode are combined into a curve that represents the global decay of sound in the room. This decay curve is not a straight line, and thus the choice of evaluation range is crucial for the value assigned to the reverberation time, e.g. the range from −5 to −25 dB for the T_{20} reverberation time.

The second part of this paper deals with the effect of non-parallel walls and diffusing elements to control flutter echoes and the reverberation time. The problem of sound decay at low frequencies and the interaction of modes with different reverberation times have been analysed by many authors, e.g. Hunt *et al.* [7] looking at rectangular rooms, while Kuttruff and Strassen [8] included rooms with non-parallel walls. Van Nieuwland and Weber [9] found that the natural frequencies of the room modes changed slightly up or down when a wall was angled a few degrees compared to the room with parallel walls. Other early papers on flutter-echoes and the effect of non-parallel surfaces include Maa [10], Kraut and Bücklein [11], and Kuhl [12].

A new method called *modal energy analysis* is suggested to calculate the effect of angled walls and scattering surfaces. The basic principle is that the reflection from a surface that is not exactly perpendicular to the incident wave will give energy transfer to other room modes; primarily from the powerful axial modes to the less powerful tangential and oblique modes. This energy can be quantified if the directivity pattern of the reflection from a rectangular surface is known.

Models for the scattering from rough surfaces have previously been published by Embrechts *et al.* [13, 14, 15]. The surfaces that have been studied are random surfaces, sine-shaped surfaces and periodic rectangular surfaces. In this paper a simple model for the scattering from geometrical structures with wedge shape or pyramidal shape is presented.

2. Frequency response of a room at low frequencies

2.1. Normal modes of a rectangular room

The model is based on a simple, rectangular room with the dimensions l_x, l_y and l_z. Later this model will be modified by allowing the surfaces to be moderately tilted. The sound absorption coefficients of the six surfaces are α_{x1}, α_{x2}, α_{y1}, α_{y2}, α_{z1} and α_{z2}. The well-known solution to the wave equation yields the natural frequency of the mode with modal numbers (n_x, n_y, n_z) [16, Eq. (3.16)],

$$f_n = \frac{c}{2}\sqrt{\left(\frac{n_x}{l_x}\right)^2 + \left(\frac{n_y}{l_y}\right)^2 + \left(\frac{n_z}{l_z}\right)^2}, \tag{1}$$

and the modal shape function for the sound pressure [16, Eqn. (3.15)]

$$\Psi_n(x, y, z) = \cos\frac{\pi x n_x}{l_x}\,\cos\frac{\pi y n_y}{l_y}\,\cos\frac{\pi z n_z}{l_z}. \tag{2}$$

2.2. Modal energy and decay rate of a single mode

The modal energy is calculated by considering a *representative wave*, i.e. a propagating sound wave that is reflected from the surfaces in accordance with the modal number. Thus, an axial mode with mode number $(n_x, 0, 0)$ propagates back and forth between the end walls and includes only the absorption from the two surfaces perpendicular to the x-axis, and the corresponding representative wave will include the two absorption coefficients α_{x1} and α_{x2}.

In the case of a tangential mode, four surfaces are involved and the respective absorption coefficients contribute to the attenuation of the mode with different weights, depending on the actual mode number. Some examples of two-dimensional room modes and corresponding representative waves are shown in Figure 1. For the mode (1,2) the representative wave includes the absorption coefficients α_{x1} and α_{x2} with the weight of 1, and α_{y1} and α_{y2} with the weight of 2. For a room mode in general, the representative wave has N reflections,

$$N = 2\left(n_x + n_y + n_z\right). \tag{3}$$

This is the necessary and sufficient number of reflections to consider, in order to calculate the contributions from all surfaces with a correct weighting. The total length of propagation of the representative wave for mode n is

$$l_{N,n} = 2\sqrt{\left(l_x n_x\right)^2 + \left(l_y n_y\right)^2 + \left(l_z n_z\right)^2}. \tag{4}$$

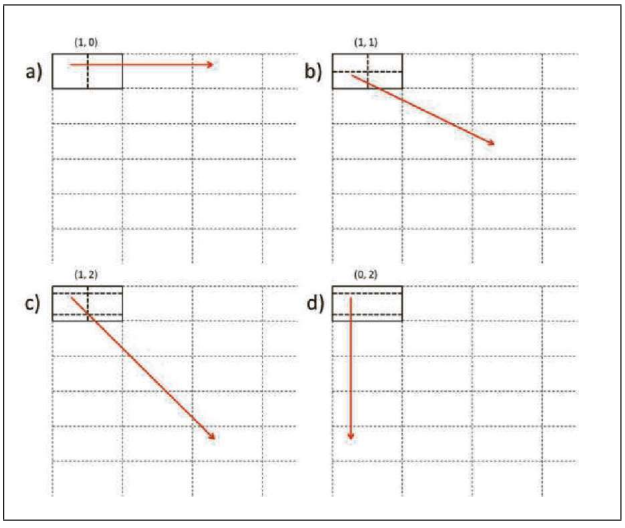

Figure 1. Examples of two-dimensional room modes and representative waves; a) axial mode (1, 0); b) tangential mode (1, 1); c) tangential mode (1,2); d) axial mode (0, 2). The representative waves (arrows) travel through the image rooms shown in dotted lines.

The energy of the wave is reduced at each reflection by the factor 1 minus absorption coefficient of the surface. Thus, the energy after N reflections is

$$E_{N,n} = E_0\left[\left(1-\alpha_{x1}\right)\left(1-\alpha_{x2}\right)\right]^{n_x} \cdot \left[\left(1-\alpha_{y1}\right)\left(1-\alpha_{y2}\right)\right]^{n_y} \cdot \left[\left(1-\alpha_{z1}\right)\left(1-\alpha_{z2}\right)\right]^{n_z}, \quad (5)$$

where E_0 is the initial energy. Hence, the modal energy takes both the absorption coefficients and the mode number into account. The effect of air attenuation can easily be included by multiplying with $\exp(-ml_{N,n})$ where m is the air attenuation factor [16, p. 70], but since we are only considering low frequencies in small rooms this effect is negligible and not included.

The reverberation time of mode n is calculated by a method similar to the derivation of the Eyring equation [16, Eq. 3.30], but instead of using the mean free path and the mean absorption coefficient, the total path for the N reflections of the representative wave and the absorption coefficients of each surface are used,

$$T_n = \frac{13.8 l_{N,n}}{-c\ln\left(E_{N,n}/E_0\right)}, \quad (6)$$

where c is the speed of sound.

Insertion of the above equations yields the reverberation time of a specific room mode (n_x, n_y, n_z):

$$T_n = 13.8\cdot 2\sqrt{\left(l_x n_x\right)^2+\left(l_y n_y\right)^2+\left(l_z n_z\right)^2} \cdot\left[-c\ln\left(\left[\left(1-\alpha_{x1}\right)\left(1-\alpha_{x2}\right)\right]^{n_x} \cdot\left[\left(1-\alpha_{y1}\right)\left(1-\alpha_{y2}\right)\right]^{n_y} \cdot\left[\left(1-\alpha_{z1}\right)\left(1-\alpha_{z2}\right)\right]^{n_z}\right)\right]^{-1}. \quad (7)$$

The above derivation is based on the representative wave with N reflections. We could continue and follow the representative wave up to $2N$ reflections or any multiple q of N; then the length of propagation is q times longer, but at the same time the energy is attenuated by the power of q. So, the derived reverberation time of the room mode remains the same (7).

The method of the representative wave implies that axial modes in one direction have the same reverberation time independent on the mode number, under the assumption that absorption coefficients do not change with frequency and no scattering effects. The latter will be dealt with later in section 3. The method also implies that a tangential mode like (9, 1, 0) has a reverberation time very close to that of the axial mode (9, 0, 0) because the absorption coefficients of the y-surfaces have little weight (1/9) compared to the absorption coefficients of the x-surfaces. The frequency response of a single room mode is given by [17, p. 63]

$$E_n(\omega) = \frac{|A_n|^2}{(\omega^2-\omega_n^2)^2+4\omega^2\delta_n^2}, \quad (8)$$

where A_n is the amplitude of the mode. The angular frequency is: $\omega = 2\pi f$ and the natural angular frequency of mode n is $\omega_n = 2\pi f_n$.

The damping constant δ_n of mode n is

$$\delta_n = \frac{3}{\log e\, T_n} \simeq \frac{2.2\pi}{T_n} = \pi B_{r,n}, \quad (9)$$

where T_n is the reverberation time and $B_{r,n}$ is the 3 dB bandwidth (in Hz) for each mode [17, eqs. III.31 and III.37].

If the sound field is excited by a sound source in the position (x_0, y_0, z_0) the response of the room is frequency dependent and the modal shape function (2) applies. Similarly, with a receiver in position (x, y, z), the sound pressure varies with frequency as given by the modal shape function in that position. The result is that the steady state energy in the point-to-point transfer function of a mode is

$$|A_n|^2 = E_{N,n}\,\Psi_n^2(x,y,z)\,\Psi_n^2(x_0,y_0,z_0), \quad (10)$$

where the mode shape function takes into account the source position (x_0, y_0, z_0) and the receiver position (x, y, z).

In the following the mode shape functions will be set to unity, which is equivalent to assuming source and receiver positions in (different) corner positions. In this way it is assured that all modes are included in the transfer function, and this is the best choice for a general evaluation of the frequency response of a room. For comparison a receiver position in the room centre is also applied in some examples.

2.3. The pressure chamber mode

Special consideration is needed for the very first room mode $(n_x, n_y, n_z) = (0, 0, 0)$ for which the room acts as

a pressure chamber with the same sound pressure over the entire volume. It is only partly a resonant mode because the natural frequency is zero, and it is hard to imagine a reverberation time associated with this mode. On the other hand, the mode represents a physical state of energy with a damping constant.

The mode is neither axial nor tangential, but can be considered a member of the same family of modes as the oblique modes with equal modal numbers, $i = n_x = n_y = n_z$. For these modes the length of propagation of the representative wave is

$$l_{N,n=i} = 2i\sqrt{l_x^2 + l_y^2 + l_z^2}, \tag{11}$$

and the energy after N reflections of the representative wave is

$$E_{N,n=i} = E_0\Big[\big(1-\alpha_{x1}\big)\big(1-\alpha_{x2}\big)\big(1-\alpha_{y1}\big) \cdot \big(1-\alpha_{y2}\big)\big(1-\alpha_{z1}\big)\big(1-\alpha_{z2}\big)\Big]^i. \tag{12}$$

The damping constant is

$$\begin{aligned}\delta_n &= \frac{3}{\log e\, T_n} \simeq -c\frac{\ln\left(E_{N,n=i}/E_0\right)}{2l_{N,n=i}} \\ &= -c\ln\Big[\big(1-\alpha_{x1}\big)\big(1-\alpha_{x2}\big)\big(1-\alpha_{y1}\big) \cdot \big(1-\alpha_{y2}\big)\big(1-\alpha_{z1}\big)\big(1-\alpha_{z2}\big)\Big] \\ &\quad \cdot \left[4\sqrt{l_x^2 + l_y^2 + l_z^2}\right]^{-1}.\end{aligned} \tag{13}$$

It is seen that i disappears from the equation, and thus the damping constant is the same for all modes in this group (as long as the absorption coefficients do not change with frequency). For the first room mode, $i = 0$, the energy is $E_{N,n} = E_0$ and the damping constant is given by equation (13).

2.4. Global frequency response

The frequency response taking all modes into account is found by summation of the modal energies (8)

$$E_n(\omega) = \sum_n \frac{|A_n|^2}{(\omega^2 - \omega_n^2)^2 + 4\omega^2\delta_n^2}. \tag{14}$$

In a music practice room neither the source position nor the receiver position are well defined, and therefore it is suggested to consider only the global frequency response, representing the total acoustic energy in the room as a function of frequency. This implies that the interference effect is neglected and the mode shape functions are set to unity; thus $|A_n|^2$ is replaced by $E_{N,n}$ in the equation above.

The calculated global frequency response is shown in Figure 2 for a rectangular example room with dimensions $(l_x, l_y, l_z) = (4.32\,\text{m}, 3.38\,\text{m}, 2.70\,\text{m})$ and absorption coefficients $(\alpha_{x1}, \alpha_{x2}, \alpha_{y1}, \alpha_{y2}, \alpha_{z1}, \alpha_{z2}) = (0.05, 0.05, 0.10, 0.10, 0.15, 0.80)$. The volume is 39 m^3 and ratio of dimensions 1.6:1.25:1. The frequency response may vary considerably if the receiver position is not in a corner, but somewhere else in the room. In order to indicate the approximate range of variation, the rather extreme frequency response in a receiver position in the room centre is also shown in Figure 2. In this position all the modes with an uneven number n_x or n_y or n_z are eliminated; so, the first peak is at the mode $(2, 0, 0)$.

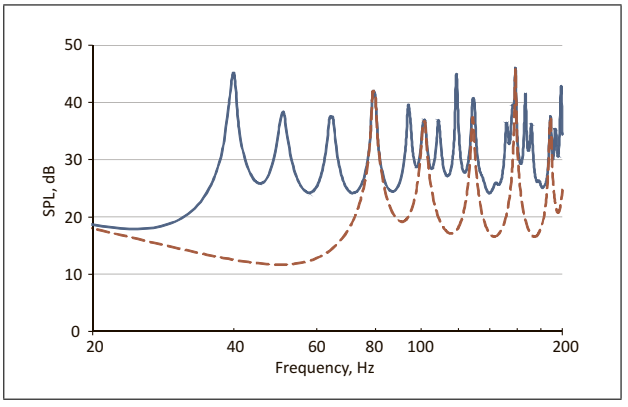

Figure 2. Example of calculated frequency responses for a 39 m^3 rectangular room with the ratio of dimensions 1:1.25:1.60. Full line is the global frequency response. The dashed curve is calculated for a receiver in the room centre.

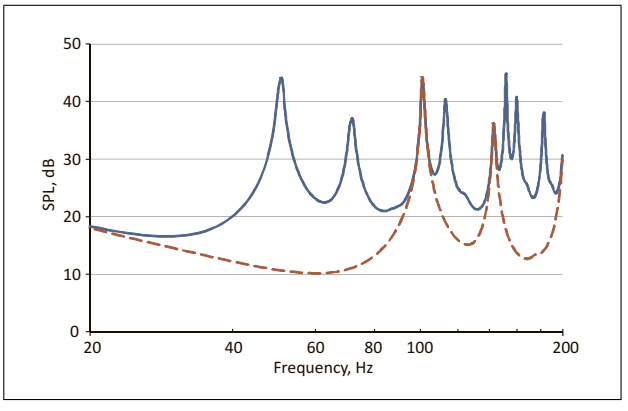

Figure 3. Example of calculated frequency responses for a 39 m^3 cubical room. Full line is the global frequency response. The dashed curve is calculated for a receiver in the room centre.

In order to illustrate the importance of appropriate ratios of room dimensions, the global frequency response for a cubical room with same volume and same absorption coefficients is shown in Figure 3. The advantage of choosing appropriate room dimensions is obvious by comparing Figure 2 and 3.

The difference between the two room examples can also be seen in relation to the sound produced by a musical instrument. Considering the musical tones in the three lowest octaves of a piano, i.e. from A0 (27.5 Hz) to A3 (220 Hz). The room with preferred dimension ratios has a good distribution of the modal frequencies. The octave between A2 and A3 is fully supported and in total 21 tones are represented within this range, see Figure 4. This is in contrast to the cubic room with same volume as displayed in Figure 5. Only 13 tones are represented, and in the octave between A2 and A3 there are several tones missing. For a music

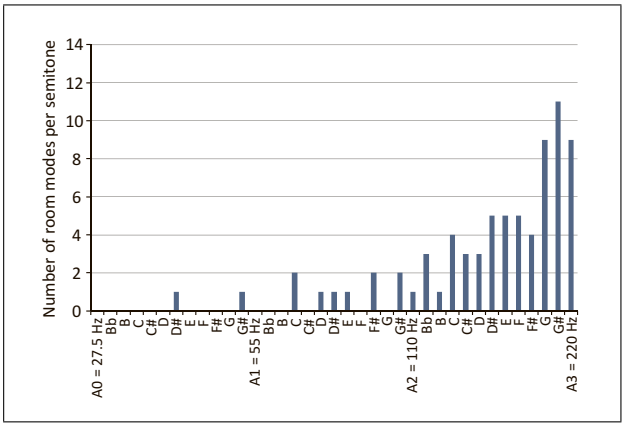

Figure 4. Distribution of room modes on the musical scale from A0 to A3 in the 39 m^3 room with dimension ratio 1:1.25:1.6. In this room 21 of 37 notes are supported by the room modes.

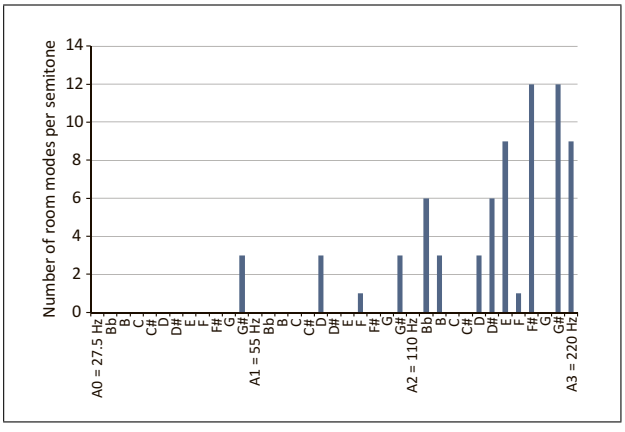

Figure 5. Distribution of room modes on the musical scale from A0 to A3 in the 39 m^3 cubical room. Only 13 of 37 notes are supported by the room modes.

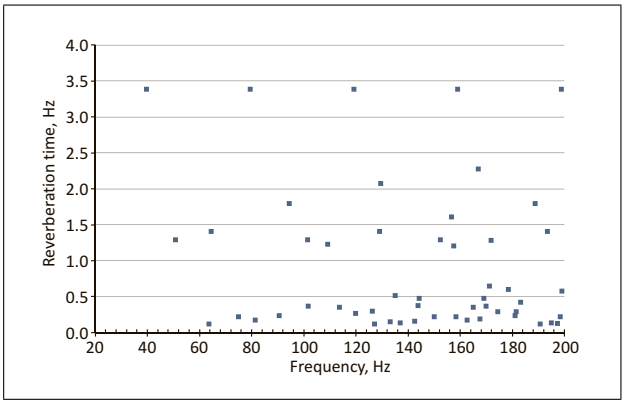

Figure 6. Reverberation times of the individual modes. The room is the same as in Figure 2.

practice room there is no doubt which room is the better one.

2.5. Reverberation within a frequency band

The reverberation time of each mode is calculated as shown in Figure 6 for the same example room as used in Figure 2. Table I shows the results for the first 14 modes. It is seen that the reverberation times varies a lot, from 3.4 s in the axial modes along the x-axis down to 0.1 s. The first oblique mode also has a short reverberation time of 0.2 s. Within the 63 Hz octave band (between 44.7 and 89.1 Hz) there are six modes, whose individual decay curves are shown in Figure 7a. When these decay curves are added (on energy basis) the resulting decay curve is bent as shown in Figure 7b. The suggested straight line approximation yields a result of 3.1 s, but it is obvious that there

Table I. The first 14 modes and their natural frequencies and reverberation times for the same room as in Figure 2.

n_x	n_y	n_z	f_n [Hz]	T_n [s]
1	0	0	39.7	3.4
0	1	0	50.8	1.3
0	0	1	63.6	0.1
1	1	0	64.5	1.4
1	0	1	75.0	0.2
2	0	0	79.5	3.4
0	1	1	81.4	0.2
1	1	1	90.6	0.2
2	1	0	94.3	1.8
0	2	0	101.6	1.3
2	0	1	101.8	0.4
1	2	0	109.1	1.2
2	1	1	113.7	0.4
3	0	0	119.2	3.4

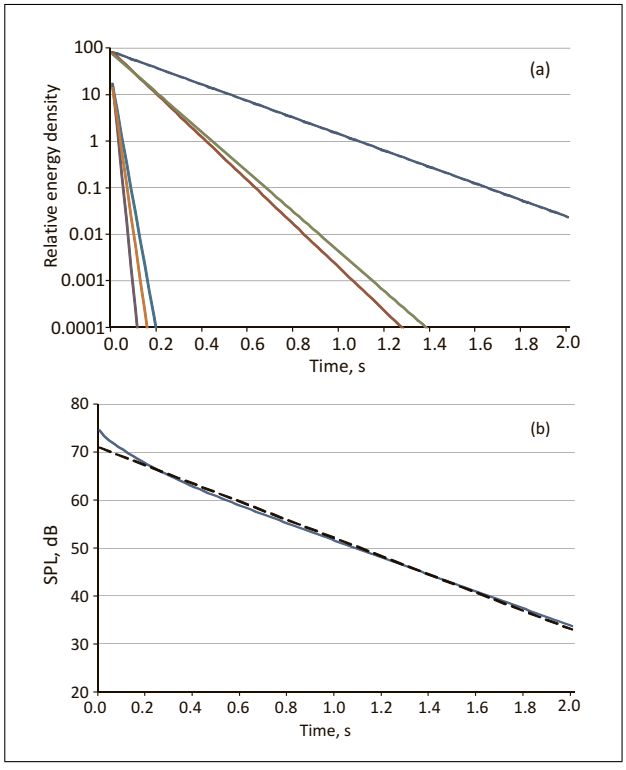

Figure 7. Calculated decay curve from the six modes within the 63 Hz octave band. a) decay of individual modes. b) averaged decay curve. The dotted line is a straight line regression with a reverberation time of 3.1 s.

is some uncertainty on the reverberation time in this example, and the result may change with position because the modes will have different weight in different positions. This is typical of an empty rectangular room with insufficient diffusion.

3. Modal energy analysis

3.1. Coupling between modes due to scattering

The modal energy analysis (MEA) implies that each mode is considered a resonant system. The modes in a rectangular room can be divided into seven groups: Three groups of axial modes, three groups of tangential modes and one group of oblique odes. The possible coupling between these groups is shown in the diagram in Figure 8. It is assumed that a physical precaution for possible exchange of energy between two modes is that they have one geometrical dimension in common. In other words, the modes must have one pair of room surfaces in common in order to have the possibility to exchange energy. For example energy can be transferred from the axial mode in the x-direction to the tangential mode in the x-y-direction if one of the end walls is angled along the z-direction. Similarly, the energy can be transferred to the tangential mode in the x-z-direction if one of the end walls in the x-direction is tilted along the y-direction. However, for geometrical reasons the tangential mode in the y-z-direction cannot couple to the axial mode in the x-direction because they have no reflecting surfaces in common. The three groups of tangential modes are orthogonal and thus it is assumed that a coupling between them is unlikely, or in any case very weak, and this is not shown in Figure 8. Coupling from axial or tangential modes to oblique modes is possible, and this is shown as dotted lines in Figure 8.

The energy transfer between two modes is possible if (1) there is a physical connection allowing the energy transfer as described above, and (2) the natural frequencies of the two modes are sufficiently close, preferably within the 3 dB bandwidth of the modes. Both conditions must be fulfilled. The second condition can be explained by considering each mode as a resonant system with one degree of freedom; the transfer function has a peak at the resonance frequency and decreases towards lower and higher frequencies, see (8). The transfer function describes the ability to deliver energy to other systems or to receive energy from other systems, and thus the coupling between two modes is weak when the resonance frequencies are far away, but it can be strong between modes with resonance frequencies close to each other.

The latter is not very likely to be fulfilled in small rooms at low frequencies; however, the coupling to another mode is always possible, but the coupling is weaker when the natural frequencies of the two modes are far away. For obvious physical reasons, the energy transfer goes from the mode with higher energy to the mode with lower energy, like in SEA [16, p. 328-329]. So, the stronger axial modes can deliver energy to the weaker but more numerous tangential and oblique modes. These coupling losses

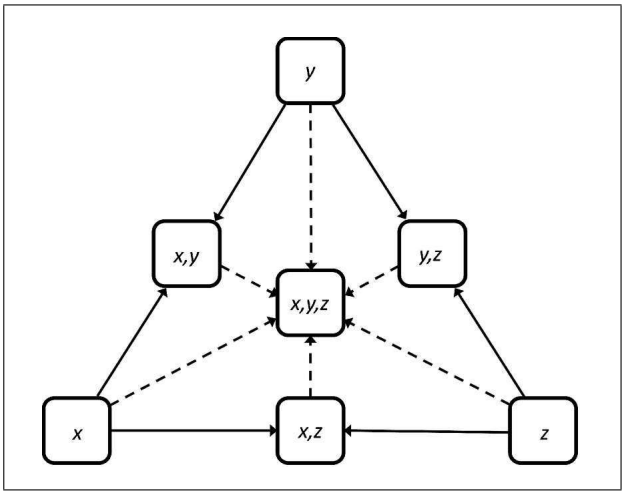

Figure 8. Diagram for modal energy analysis of room modes; axial modes (1-dimensional), tangential (2-dimensional) and oblique (3-dimensional). Energy transfer is always from the stronger to the weaker modes.

can be described by the scattering coefficients of the surfaces, both in case of diffusors and for angled surfaces as described in the following.

3.2. The modal scattering coefficient

The scattering coefficient s of a reflecting surface is usually defined as the fraction of reflected energy in directions different from the direction of the specular reflection; thus $(1 - s)$ is the fraction of reflected energy in the specular direction. However, for the purpose of modal energy analysis a slightly different definition applies: In an axial mode $(1 - s)$ is the fraction of reflected energy that remains in the axial mode. Thus, s is here the fraction of reflected energy transferred to higher order modes and this is named the *modal scattering coefficient*.

In the case of an axial mode with mode number $(n_x, 0, 0)$ the energy in the mode after N reflections is

$$E_{N,n} = E_0 \Big[\big(1 - \alpha_{x1}\big)\big(1 - s_{x1}\big) \big(1 - \alpha_{x2}\big)\big(1 - s_{x2}\big) \Big]^{n_x}, \qquad (15)$$

and similarly for the axial modes in the y- and z-directions.

In the calculation model the scattered energy is treated as absorbed energy, i.e. the energy is lost in the relevant axial mode, but as an approximation and for simplicity it is not transferred to any other mode in the present calculation model. This implies an error, which is assumed to be insignificant. In order to explain this we can look at the example in Table I and the decay curves within an octave band shown in Figure 7. The strongest mode is $(2, 0, 0)$ with reverberation time 3.4 s; this can couple to the tangential modes $(1, 1, 0)$ with $T = 1.4$ s and $(1, 0, 1)$ with $T = 0.2$ s. In case of coupling between these modes, the tangential modes could have some increase in reverberation time, but the decreased reverberation time of the axial mode is much more important, because the weaker modes contributes very little to the total result.

3.3. Flutter echo and the effect of tilting a wall

The effect of tilting a wall by an angle θ is shown in Figure 9. Due to the finite size of the wall the reflected energy is scattered and the maximum energy is reflected in the specular direction, i.e. away from the direction of sound propagation in the axial mode. The question is how much energy is reflected back in the direction of the axial mode.

The reflection pattern for a rectangular surface has been analysed in [18] and it is shown that the result for the 3D reflection pattern is orthogonal, i.e. it is the product of the 2D reflection patterns valid for the length and the width of the surface. An example of the 2D reflection pattern for a surface with the width $2a$ (and infinitely long) is shown in Figure 10. If the sound is incident from the angle α_0 the ratio of energy reflection I_α in the direction α to the reflection in the specular direction $I_{\alpha 0}$ is [18]:

$$\frac{I_\alpha}{I_{\alpha 0}} = \left(\frac{\sin X}{X}\right)^2, \tag{16}$$

where

$$X = ka\big(\cos\alpha - \cos\alpha_0\big) \to 2ka\sin\theta, \tag{17}$$

and $k = 2\pi f/c$. In order to apply the result to the present case of modal scattering, we set $\alpha = \pi - \alpha_0$. The wall is tilted the angle θ, so $\alpha_0 = \pi/2 - \theta$ and $\alpha = \pi/2 + \theta$. The fraction of reflected energy staying in the axial mode is

$$1 - s = \left(\frac{\sin\big(2ka\sin\theta\big)}{2ka\sin\theta}\right)^2, \tag{18}$$

where s is the modal scattering coefficient representing the fraction of reflected energy leaving the axial mode.

Very detailed investigations and scale model measurements of the reverberation time of axial modes between two surfaces in an anechoic environment were reported by Krauth and Bücklein [11]. The effect of tilting one wall was investigated, among other things. A similar experiment has been made with the new MEA model, using 2.5 m wide walls with a distance of 3.0 m, which means that a scale factor of 1:10 is assumed for the experimental data. The absorption coefficients of the two opposing walls were set to 0.15 in order to obtain the same reverberation time as measured with parallel walls. The angle of one wall was changed in steps of 1° up to 20° and the reverberation times of each mode was calculated.

Figure 11 shows the calculated reverberation time of the four selected modes as functions of the angling of one wall. In the scale model experiments it is not clear which frequency range was actually measured; no frequency band filtering was mentioned, but the sound source was a spark source with a limited bandwidth. The calculated results between 343 and 458 Hz are very close to the measured results up to 3°; for larger angles the measured reduction of the reverberation time corresponds to that calculated for lower frequencies. This may be explained by the fact that the high frequencies are attenuated more than

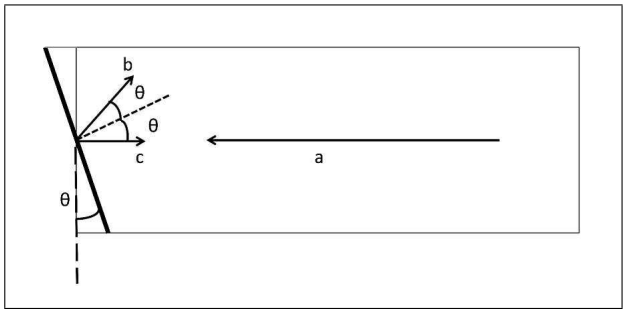

Figure 9. Reflection from wall tilted by the angle θ. a: incident sound in axial mode, b: maximum reflection in specular direction, c: reflection in direction of the axial mode.

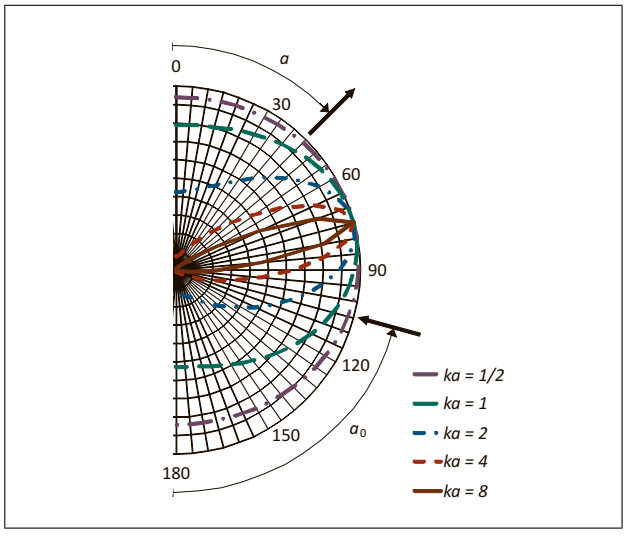

Figure 10. Refelction pattern for a plane wave incident on a surface with the width $2a$.

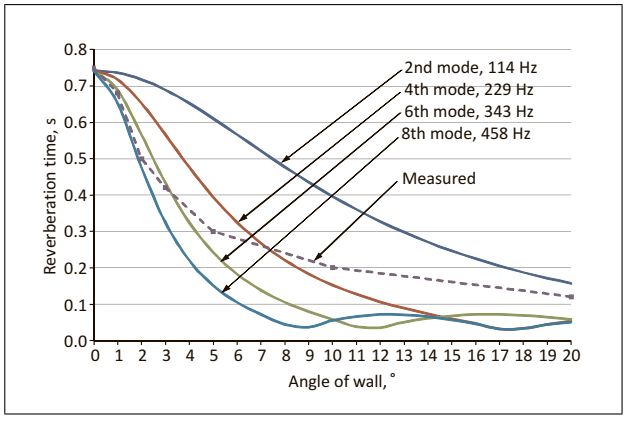

Figure 11. Reverberation time for axial modes as a function of wall angle. The walls are 2.5 m wide and 3.0 m apart. Measured data are from [11].

the lower frequencies by the angled wall, and thus the measured sound energy is shifted towards lower frequencies when the angle is increased. However, since the measured data are wideband (unspecified), the comparison with calculated results for single frequencies can only give an in-

dication and cannot be taken as a final validation of the calculation model.

It appears that for the chosen dimensions and distance, an angle of 5° is sufficient to reduce the reverberation time at frequencies above ca. 300 Hz to values less than half the reverberation time with parallel walls, and thus the flutter echo should be practically eliminated.

3.4. Scattering due to wedge-shaped structures

The result above can be further developed considering the angled wall to be subdivided into many surfaces, all having the same angle θ relative to the plane of the wall, see Figure 12. In this case it is more practical to characterize the scattering structure by the total depth $2d$ of the structure (the roughness) instead of the angle. Thus, setting $2a \sin\theta = 2d$ we get the modal scattering coefficient for a 1D diffuser with wedge-shaped structures,

$$s = 1 - \left(\frac{\sin 2kd}{2kd}\right)^2 \simeq \frac{(2kd)^2}{3} - \frac{(2kd)^4}{36}, \qquad (19)$$

where the approximation is the first two terms of the Taylor series. With this change of parameter the scattering surface is characterized by the roughness in terms of the total depth of the structure, and the modal scattering coefficient is identical to the normal incidence scattering coefficient of the surface.

Considering a 2D diffuser with pyramid-shaped structures, this is an orthogonal problem and the reflection in the direction of the axial mode is attenuated twice by the factor $(1-s)$. This leads to the normal incidence scattering coefficient of the 2D diffuser,

$$s = 1 - \left(\frac{\sin 2kd}{2kd}\right)^4 \simeq \frac{2(2kd)^2}{3} - \frac{(2kd)^4}{9}. \qquad (20)$$

It is seen that $s \to 1$ for $kd \to \infty$, and $s \to 0$ for $kd \to 0$. Again the approximation shows the first two terms of the Taylor series and is valid for $2kd < 1$. In both cases (19) and (20) the scattering coefficient increases with the second power of the frequency, but the 2D diffuser has approximately twice as high scattering as the 1D diffuser with the same total depth. The results derived here can be compared to that for a random rough surface, where the "average Gausian" model in [13] leads to the normal incidence scattering coefficient,

$$s = 1 - \exp\left(-(2k\sigma)^2\right) \simeq (2k\sigma)^2 - (2k\sigma)^4/2, \qquad (21)$$

where σ is the rms height of the structure and the approximation is the first two terms of the Taylor series. For the 1D wedge-shaped diffusor $\sigma = d/3$. This means that with the same total height (or depth) of the structure, the normal incidence scattering coefficient of the 1D wedge-shaped diffusor is about three times higher than of a random rough surface. It would be interesting to compare the random incidence scattering of different structures, but this is outside the scope of this paper.

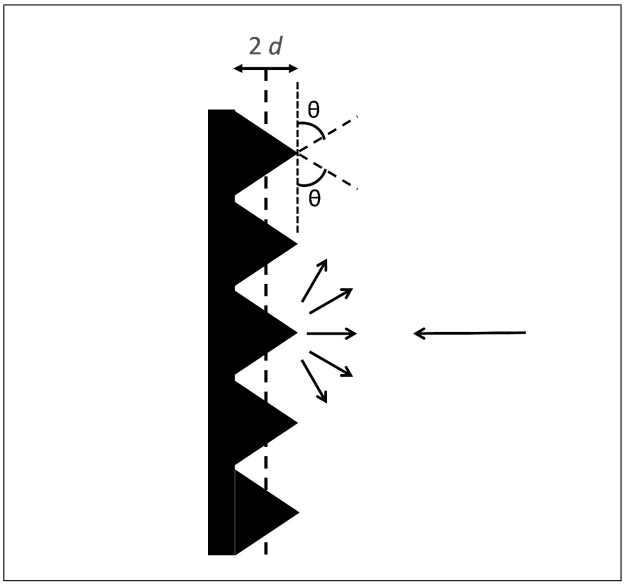

Figure 12. Scattered reflection from a wedge shaped diffusor.

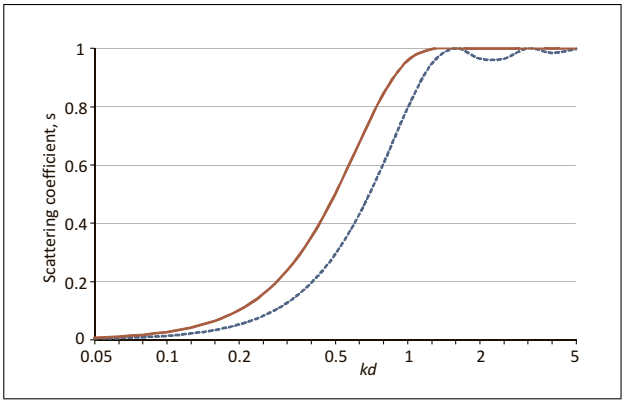

Figure 13. Scattering coefficients as function of kd, where $2d$ is the total roughness of the structure. The solid and dashed lines show results for the 2D and 1D diffusers, respectively.

The scattering coefficients are shown as functions of kd in Figure 13. For comparison, the default mid-frequency scattering coefficient in some room acoustic calculation programs is $s = 0.05$. At 707 Hz (centre frequency of the octave bands 500 and 1000 Hz) we have $k = 12.7\ \mathrm{m}^{-1}$ and thus the corresponding structural depth $2d$ is around 2 or 3 cm for a 2D or 1D diffuser, respectively.

Experimental results of a scattering structure are also reported by Krauth and Bücklein [11]. Starting with two parallel walls (0.6 m × 0.8 m) in a distance on 1.0 m, they measured the reverberation time of the axial mode and the effect of treating one wall with convex half-spheres, the radius of which was varied. Assuming a scale factor of 1:10, the distance between the walls is 10 m and the total roughness is varied from 0 to 0.9 m. In the MEA model the absorption coefficient of the walls is set to 0.09 in order to get the same reverberation time as measured without any scattering treatment. The results are shown in Figure 14. The measured results agree with the calculated results around 137 Hz for little roughness, while the results

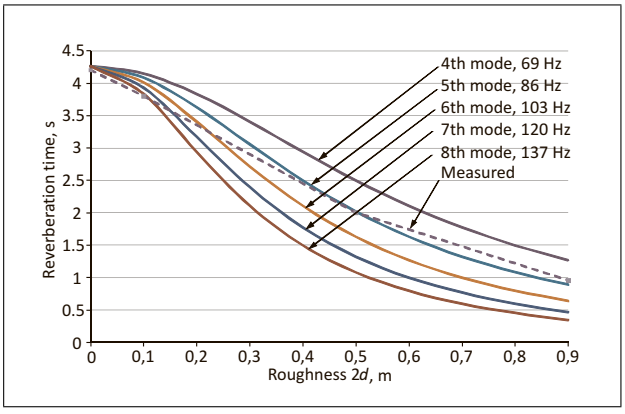

Figure 14. Reduction of reverberation time due to a scattering structure as a function of surface roughness. The walls are 6 m × 8 m and 10 m apart. Measured data are from [11].

for larger roughness show better agreement with calculations around 86 Hz. As in the case of the tilted wall discussed above, this frequency shift may be due to the fact that no frequency filtering was applied to the measurements.

4. Example

A music practice room described by D'Antonio and Cox [19] is applied for this example. The dimensions are 4.5 m long, from 2.1 m to 2.4 m wide (one wall angled), and 2.7 m high, see sketch in Figure 15. A 2D hybrid diffuser-absorber is mounted on one wall (A in Figure 15), and the ceiling is treated with a 2D diffusor. Measured frequency responses and reverberation times are reported for the situations before and after one of the end walls was treated with an acoustical masonry block that provided 1D diffusion and some low frequency absorption (B in Figure 15).

From the description in [19] it is estimated that the roughness of the masonry blocks and ceiling structures are $2d = 0.20$ and 0.30 m, respectively. Absorption coefficients in the low frequency region are estimated from the description of the materials. The masonry blocks are assumed to change the low frequency absorption coefficient around 63 Hz from 0.1 to 0.25. The calculated global frequency responses before and after the addition of the masonry blocks are shown in Figure 16. The measured frequency response after treatment reported in [19] is also shown for comparison. The frequency response of the loudspeaker is not known, but the somewhat higher levels measured above 50 Hz may be due to the response of the loudspeaker. The measured fluctuations between 20 and 30 Hz may also be due to the loudspeaker and not the room. Despite from this, the calculated curves are in satisfactory agreement with the measured frequency response.

The calculated reverberation times of the individual modes before and after the treatment are listed in Table II. Since the treated wall is the end wall in the x-direction, only modes with $n_x > 0$ are affected, and the axial modes are attenuated most. The 63 Hz octave band contains five

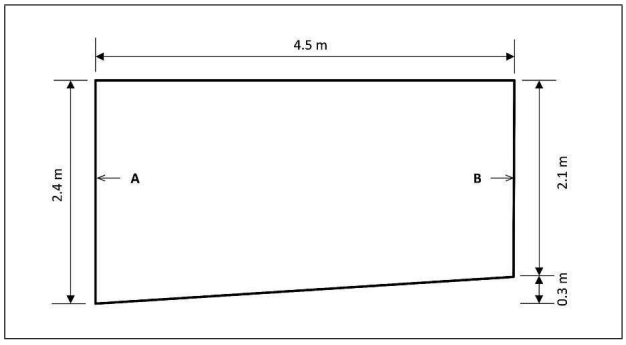

Figure 15. Plan of music practice room. A is a 2D hybrid diffuser and B is the wall treated with acoustical masonry blocks. The room height is 2.7 m.

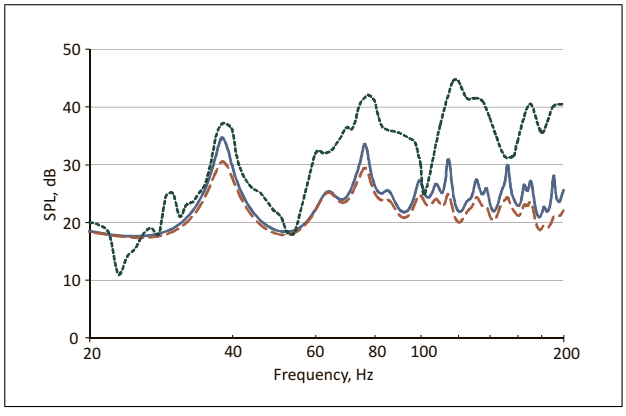

Figure 16. Global frequency responses for example room calculated by modal energy analysis. Full line: before treatment. Dashed line: after treatment of wall. Dotted line: Measured frequency response after treatment [19].

modes with natural frequencies from 63.6 to 85.3 Hz. The reverberation time is dominated by the axial mode (2, 0, 0) at 76.3 Hz, and this is the mode which is most affected by the introduction of the masonry blocks. The calculated 63 Hz octave band decay curves are shown in Figure 17. The octave band reverberation time is calculated to be shifted from 0.88 s to 0.58 s by the treatment, which is in close agreement with the measurement results [19, Fig. 25].

5. Discussion

The modal energy analysis (MEA) is based on some assumptions concerning the energy of the modes and the coupling between modes. The room has six surfaces, each with its own absorption coefficient. The method developed for calculating the damping of the room modes is the representative wave, which is introduced as a means to find the contribution of the absorption coefficients of the six surfaces. While the answer to this is obvious for the axial modes, this is not a simple question for the tangential and oblique modes. From traditional wave based room acoustics it is known that a tangential mode can be considered the result of four plane wave fields propagating in differ-

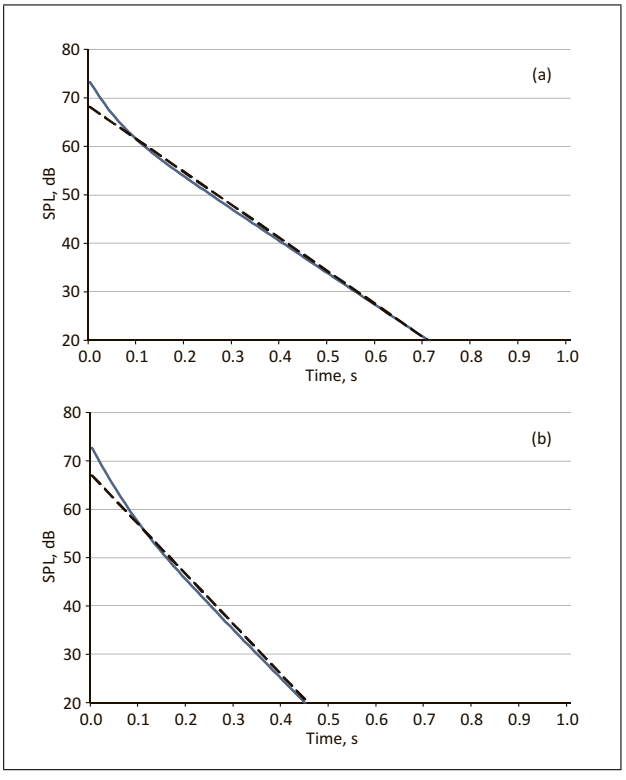

Figure 17. Calculated decay curves in the 63 Hz octave band, a) before treatment, b) after treatment of wall.

Table II. Calculated modes, natural frequencies, and reverberation times before (a) and after (b) treatment of one wall in example room.

n_x	n_y	n_z	f_x [Hz]	T_n (a) [s]	T_n (b) [s]
1	0	0	38.1	0.9	0.6
0	0	1	63.6	0.3	0.3
1	0	1	74.1	0.4	0.4
0	1	0	76.3	0.2	0.2
2	0	0	76.3	0.9	0.6
1	1	0	85.3	0.4	0.3
0	1	1	99.3	0.2	0.2
2	0	1	99.3	0.5	0.4
1	1	1	106.4	0.3	0.2
2	1	0	107.9	0.5	0.4
3	0	0	114.4	0.9	0.6

ent directions, and similarly eight propagating waves in the case of an oblique mode [19, eq. III.19]. These waves represent the phase speed, not the propagation of energy, and the associated directions of propagation cannot be used to find the contribution of absorption from the surfaces. One simple example will show this; according to the MEA model, the tangential mode (1, 1, 0) has equal contribution of absorption from the four surfaces in the x-y-plane, independent of the room dimensions, and intuitively this makes sense. But, unless it is a square room, the directions of the phase speeds will give more hits to one pair of surfaces than to the other pair, and thus an uneven weight of absorption from the four surfaces.

The room modes have been divided into seven groups and the coupling between modes in different groups has been considered, however with some approximations for simplicity. Due to the fact that the axial modes have the longest paths between reflections, they are the dominating groups of modes in the frequency response as well as in the decaying sound field. When an axial mode couples to one or more tangential modes, the loss of energy in the strong axial mode is very important, whereas the corresponding increase of energy in the relatively weak tangential modes is neglected in the present version of the model. The coupling between tangential and oblique modes is also neglected for simplicity, and this may cause some minor errors in the calculated reverberation times. However, compared to the uncertainty assigned to the absorption data of the surfaces, the approximations in the calculations should be justified.

One limitation of the calculation model is that the room shape must be nearly rectangular, although opposite surfaces can be angled to some extent; the allowable limit is not known, possibly up to a maximum of 20°. Another drawback is that there are six and only six surfaces, and they cannot be subdivided, so each surface must be represented by one material, only.

It is suggested that the global frequency response is sufficient for designing purposes for music practice rooms where the source and receiver positions are not fixed. If desired for other purposes, it is possible to define a source position and a receiver position in the room, but some room modes may be weak or even completely missing in some positions, as demonstrated in the examples. Only the corner positions will ensure an equal balance between the room modes and thus the global frequency response is a good way to characterize the room as such.

In the current version of the MEA model the absorption coefficients are not functions of the frequency. An obvious possibility for further development is allowing the absorption coefficients to vary with frequency, or – even better – to introduce frequency dependent impedances for each surface.

6. Conclusion

The modal energy analysis (MEA) is suggested as a simple and efficient method to calculate the frequency response and reverberation time at low frequencies in small and nearly rectangular rooms.

The effect of tilting or angling a wall to prevent flutter echo is included in the model, and using a novel method the effect is quantified by a modal scattering coefficient. Angling a wall is a measure to extract energy from axial modes by coupling to other modes with less energy. The efficiency is lowest at low frequencies, but increases with the frequency. Since the strongest axial modes are usually between the end walls in the longest direction of the room, these walls should have highest priority for the angling. The effect on the natural frequencies of the room is negligible, while the effect on the frequency response is slightly lower and wider peaks at those axial modes affected by the

measure. How much angling is needed depends on the size of the wall and should be evaluated from case to case; only a few degrees may be sufficient. Actually, the suggested model shows that the important parameter is not the angle but the total variation in depth, so a small wall needs more angling than a big wall.

The effect of diffusing treatment on a surface is also included by means of a simple model for calculating the normal incidence scattering coefficient as a function of the depth of a geometrical structure with triangular wedges or pyramids.

The calculation model has been made in Excel, and the calculation time is negligible. The model is suggested as an alternative to the more time consuming FEM and BEM models for the acoustical design of small rooms, e.g. music practice rooms.

References

[1] J. E. Volkman: Polycylindrical diffusers in room acoustical design. JASA **13** (1942) 234–243.

[2] R. H. Bolt: Note on normal frequency statistics for rectangular rooms. JASA **18** (1946) 130–133.

[3] R. H. Lyon: Statistical analysis of power injection and response in structures and rooms. JASA **45** (1969) 545–565.

[4] M. M. Louden: Dimension ratios of rectangular rooms with good distribution of eigentones. Acustica **24** (1971) 101–104.

[5] O. J. Bonello: A new criterion for the distribution of normal room modes. JAES **29** (1981) 597–606.

[6] T. J. Cox, P. D'Antonio: Determining optimum room dimensions for critical listening environments: A new methodology. AES 110th Convention, Amsterdam, 2001, Convention paper 5353.

[7] F. V. Hunt, L. L. Beranek, D. Y. Maa: Analysis of sound decay in rectangular rooms. JASA **11** (1939) 80–94.

[8] H. Kuttruff, T. Strassen: Zur Abhängigkeit des Raumnachhalls von der Wanddiffusität und von der Raumform. Acustica **45** (1980) 146–255.

[9] J. M. van Nieuwland, C. Weber: Eigenmodes in nonrectangular reverberation rooms. Noise Control Engineering **13** (1979) 112–121.

[10] D. Y. Maa: The flutter echoes. JASA **13** (1941) 170–178.

[11] E. Krauth, R. Bücklein: Modelluntersuchungen an Flatterechos. Frequenz **18** (1964) 247–252.

[12] W. Kuhl: Nachhallzeiten schwach gedämpfter geschlossener Wellenzüge. Acustica **55** (1984) 187–192.

[13] J. J. Embrechts, D. Archambeau, G. B. Stan: Determination of the scattering coefficient of random rough diffusing surfaces for room acoustics applications. Acta Acustica united with Acustica **87** (2001) 482–494.

[14] J. J. Embrechts, L. De Geetere, G. Vermeir, M. Vorländer, T. Sakuma: Calculation of the random-incidence scattering coefficients of a sine-shaped surface. Acta Acustica united with Acustica **92** (2006) 593–603.

[15] J. J. Embrechts, A. Billon: Theoretical determination of the random-incidence scattering coefficients of infinite rigid surfaces with a periodic rectangular roughness profile. Acta Acustica united with Acustica **97** (2011) 607–617.

[16] Z. Maekawa, J. H. Rindel, P. Lord: Environmental and architectural acoustics. Second edition. Spon Press, London and New York, 2011.

[17] H. Kuttruff: Room acoustics. Applied Science Publishers, London, 1973.

[18] J. H. Rindel: Modelling the directional characteristics of sound reflections. Proceedings of Joint Baltic-Nordic Acoustics Meeting 2004, Mariehamn, Åland, 2004.

[19] P. D'Antonio, T. J. Cox: Diffusor application in rooms. Applied Acoustics **60** (2000) 113–142.